SEDIMENT PARTICLE SORTING ON HILLSLOPE PROFILES IN THE WEPP MODEL

D. C. Flanagan, M. A. Nearing

ABSTRACT. *The USDA-ARS Water Erosion Prediction Project is a major effort to improve estimates of soil detachment, transport, and deposition on agricultural hillslopes, as well as to estimate the amount and size distribution of the sediment leaving the field. The WEPP hillslope model computes both detachment and deposition on a total sediment load basis, though the model also estimates information on sediment particle sizes. This article describes the mathematical equations that predict the sediment particle sorting in WEPP for both interrill and rill areas on a hillslope, and presents a discussion on the advantages and disadvantages of the techniques. It also examines the amount of predicted particle sorting as affected by various model input parameters. Soil type, random roughness, rainfall intensity, slope length, slope gradient, and slope shape were all found to affect the predicted size distribution of sediment leaving a hillslope. Comparison of model results to measured data show that the technique described in this article represents the trends in sediment particle sorting observed in field experiments, with r^2 values between observed and predicted size fractions ranging from 0.44 to 0.97.*

Keywords. *Soil erosion, Sediment deposition, Sediment enrichment.*

Sediment enrichment refers to the mass fraction increase of the more chemically active fine sediment particles (silt, clay, and organic matter) due to selective deposition of coarser sediment particles (sand and large aggregates). A simple yet accurate procedure to predict the amount of particle sorting was required for the Water Erosion Prediction Project (WEPP) computer model. The procedure developed involved the use of an analytic solution to the governing sediment continuity equation, applied to an identified region of deposition on a hillslope (fig. 1). The objectives of this article are to: (1) describe the mathematical equations used in the WEPP model to estimate sediment particle sorting on interrill areas and in rills, and to explain how these functions are applied within the computer program; (2) determine the variability of sediment enrichment ratios computed by WEPP as affected by input parameters; (3) present limited validation results; and (4) discuss the advantages and disadvantages of this type of approach.

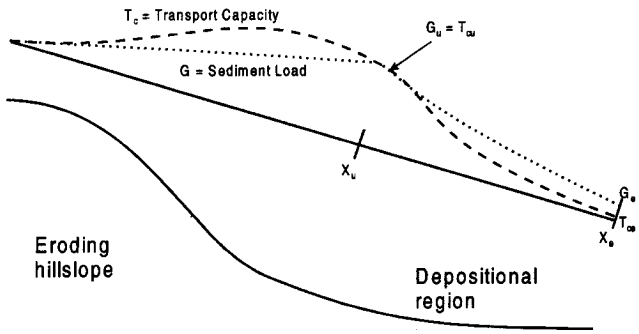

Figure 1–Idealized S-shaped hillslope showing depositional region caused by decrease of transport capacity (dashed line) below sediment load (dotted line).

BACKGROUND

The Water Erosion Prediction Project is an effort by the United States Department of Agriculture to develop improved soil erosion prediction technology based on basic physical processes (Foster and Lane, 1987). The fundamentals of infiltration, runoff, flow hydraulics, plant growth, residue decomposition, soil disturbance and consolidation, and erosion mechanics are incorporated into the WEPP computer model (Flanagan and Nearing, 1995). The main purpose of the model is to assist in natural resource planning and assessment.

A major improvement of WEPP over the Universal Soil Loss Equation (Wischmeier and Smith, 1978) is its ability to represent complex slope geometry, as well as to predict the location and amount of sediment deposition and the sediment yield from a hillslope. WEPP also allows spatial variability in land use and soil properties, which affects many processes, including hydrology, flow hydraulics, and sediment detachment, transport, and deposition. The computer model allows a hillslope to be segmented into multiple overland flow elements (OFE). An OFE is a region in which soil and management practices are homogeneous; thus, one OFE might have a silt loam soil with no-till corn on it, the next OFE could be the same soil with conventional tillage soybeans, and the next OFE could be a continuous pasture on a sandy soil.

Article has been reviewed and approved for publication by the Soil & Water Division of ASAE.

The authors are **Dennis C. Flanagan**, ***ASAE Member Engineer***, Agricultural Engineer, and **Mark A. Nearing**, Agricultural Engineer, USDA-Agricultural Research Service, National Soil Erosion Research Laboratory, West Lafayette, Indiana. **Corresponding author:** Dennis C. Flanagan, USDA-ARS NSERL, 1196 Building SOIL, West Lafayette, IN 47907-1196, phone: 765.494.7748, fax: 765.494.5948, e-mail: <flanagan@purdue.edu>.

WEPP EQUATIONS

The WEPP model uses a steady-state, sediment continuity equation to estimate net detachment or deposition:

$$\frac{dG}{dx} = D_f + D_i \quad (1)$$

where G is sediment load ($kg \cdot m^{-1} \cdot s^{-1}$), x is distance downslope (m), D_f is rill detachment rate ($kg \cdot m^{-2} \cdot s^{-1}$), and D_i is interrill sediment delivery to the rill ($kg \cdot m^{-2} \cdot s^{-1}$) (Nearing et al., 1989). Separate relationships are used for calculation of D_f depending upon whether conditions exist that will lead to detachment (transport capacity exceeds sediment load and shear stress exceeds critical shear stress) or deposition (sediment load exceeds transport capacity).

INTERRILL AREAS

The WEPP model uses an interrill sediment delivery function of the form:

$$D_i = K_{iadj} I_e \sigma_{ir} SDR_{RR} F_{nozzle} \left(\frac{R_s}{w}\right) \quad (2)$$

in which K_{iadj} is an adjusted interrill erodibility ($kg \cdot s \cdot m^{-4}$), I_e is the effective rainfall intensity ($m \cdot s^{-1}$), σ_{ir} is the interrill runoff rate ($m \cdot s^{-1}$), SDR_{RR} is the interrill sediment delivery ratio, F_{nozzle} is an adjustment factor to account for sprinkler irrigation nozzle impact energy variation and is set to a value of 1.0 for natural rainfall conditions, R_s is the spacing of the rills (m), and w is the rill width (m) (Foster et al., 1995). The variables in this equation may have different values for each overland flow element on a hillslope profile.

SDR_{RR} is computed as a function of the random roughness of the soil surface, the fall velocity of the individual particle size classes of sediment, and the particle size distribution of the sediment. This method is an adaptation of a procedure suggested by Foster (1982) and involves three steps. First, an interrill roughness factor is computed based on a functional representation of table 8.4 from Foster (1982), i.e., the interrill roughness factor is a function of random roughness of the soil surface. This factor is dimensionless, constrained within the limits of zero to one, and is computed using:

$$RIF = -23(RR) + 1.14 \quad (3)$$

where RIF is the interrill roughness factor, and RR is the random roughness of the current overland flow element (m). The range of random roughness values that can be represented by this function is thus limited to between 0.0061 and 0.0496 m (RIF of 1.0 to 0.0, respectively).

The second step is to calculate a sediment delivery ratio, DR_i, for each of the five WEPP particle size classes as a function of the interrill roughness factor and the fall velocity of the size class. The five WEPP particle size classes are primary clay, primary silt, primary sand, small aggregate and large aggregate, and their characteristics and distribution at the point of detachment are predicted as per Foster et al. (1985). The fall velocities for the individual particle size classes are calculated assuming spherical particles and standard drag relationships. The sediment delivery ratio equations used for particles with fall velocities, v_{fi}, less than 0.01 $m \cdot s^{-1}$ are as follows:

$$DR_i = az\,(RIF)^{bz} \quad (4)$$

where

$$az = \exp\left(0.0672 + 659 v_{fi}\right) \quad (5)$$

$$bz = 0.1286 + 2209\, v_{fi} \quad (6)$$

and for particles with fall velocities greater than or equal to 0.01 $m \cdot s^{-1}$ the equation is:

$$DR_i = 2.5(RIF) - 1.5 \quad (7)$$

The subscript i represents an individual particle size class. Values for DR_i are constrained between the limits of zero to one.

The third step in the procedure is to take a weighted average of the sediment delivery ratio for each particle size class, weighted by the mass fraction of sediment in each class, to obtain the total interrill sediment delivery ratio:

$$SDR_{RR} = \sum_{i=1}^{5} f_{deti}(DR_i) \quad (8)$$

where f_{deti} is the fraction of detached sediment in each size class i predicted with the Foster et al. (1985) equations. The fraction of sediment in each size class delivered from the interrill areas to the rill flow channels, $fidel_i$, is computed as:

$$fidel_i = \frac{f_{deti}(DR_i)}{SDR_{RR}} \quad (9)$$

The $fidel_i$ values are used in the updating of the flow sediment size classes at the end of each detachment region and beginning of each deposition region in the rills.

RILL AREAS

The WEPP model explicitly determines the detachment, transport and deposition in rill channels. Rill detachment is assumed to be a nonselective process, so the sediment particle size distribution generated from actively eroding areas of rills is assumed to be that predicted by the Foster et al. (1985) equation set, with adjustments made for the interrill sediment delivered to the rills. Particle sorting in rills in WEPP is predicted in depositional regions only, so only the model deposition equations will be discussed here. The governing WEPP deposition equation is:

$$D_f = \frac{\beta v_f}{q}(T_c - G) \quad (10)$$

where β is a rainfall induced turbulence factor, v_f is particle fall velocity ($m \cdot s^{-1}$), $q = q_o + \sigma x$, where q is flow discharge per unit width ($m^2 \cdot s^{-1}$), q_o is inflow per unit width ($m^2 \cdot s^{-1}$), σ is excess rainfall rate ($m \cdot s^{-1}$), T_c is sediment transport capacity ($kg \cdot m^{-1} \cdot s^{-1}$), and G is sediment load ($kg \cdot m^{-1} \cdot s^{-1}$) (Foster et al., 1995). Please refer to Foster et al. (1995), Nearing et al. (1989), and Finkner et al. (1989) for additional details related to computations and normalizations of the various terms of this equation.

Sediment load is normalized to transport capacity at the end of the OFE when there is water discharge from the OFE ($G^* = G/T_{ce}$), and is normalized to transport capacity at the top of the OFE when there is no discharge from the flow plane ($G^* = G/T_{co}$). When the deposition equation (eq. 10) is combined with the sediment continuity equation (eq. 1), the result is:

$$\frac{dG}{dx} = D_i + \frac{\beta v_f}{q}(T_c - G) \tag{11}$$

This equation can be normalized as follows:

$$\frac{d\left(\frac{G}{T_{ce}}\right)}{d\left(\frac{x}{L}\right)} = \frac{D_i L}{T_{ce}} + \frac{\beta v_f L}{q_o + \sigma x}\left(\frac{T_c}{T_{ce}} - \frac{G}{T_{ce}}\right) \tag{12}$$

$$\frac{dG^*}{dx_*} = \frac{D_i L}{T_{ce}} + \frac{\frac{\beta v_f L}{\sigma L}}{\frac{q_o}{\sigma L} + \frac{\sigma x}{\sigma L}}(T_{c^*} - G^*) \tag{13}$$

$$\frac{dG^*}{dx_*} = \frac{D_i L}{T_{ce}} + \frac{\frac{\beta v_f}{\sigma}}{x_* + q_{o^*}}(T_{c^*} - G^*) \tag{14}$$

Substituting nondimensional interrill detachment and rill deposition parameters, respectively:

$$\theta = \frac{D_i L}{T_{ce}} \tag{15}$$

$$\phi = \frac{\beta v_f}{\sigma} \tag{16}$$

reduces the equation to:

$$\frac{dG^*}{dx_*} = \theta + \frac{\phi}{x_* + q_{o^*}} T_{c^*} - \frac{\phi}{x_* + q_{o^*}} G^* \tag{17}$$

The equation for nondimensional sediment transport capacity in WEPP is:

$$T_{c^*} = A x_*^2 + B x_* + C \tag{18}$$

where A, B, and C are coefficients (see Finkner et al., 1989). Substituting this expression into equation 17 and rearranging results in the nonhomogeneous first order linear differential equation:

$$\frac{dG^*}{dx_*} + \left(\frac{\phi}{x_* + q_{o^*}}\right) G^* = \theta + \frac{\phi}{x_* + q_{o^*}}(A x_*^2 + B x_* + C) \tag{19}$$

which has an analytic solution. Equation 19 is of the form:

$$\frac{dy}{dx} + P(x)y = Q(x) \tag{20}$$

which has the general solution:

$$y = e^{-\int P(x)dx}\left(\int e^{\int P(x)dx} Q(x)dx + K\right) \tag{21}$$

(Pennisi, 1972). The specific solution for equation 19 is:

$$G^* = \left[\frac{\phi A}{\phi + 2}(x_* + q_{o^*})^{\phi+2} + \frac{(\phi B + \theta - 2A\phi q_{o^*})}{\phi + 1}(x_* + q_{o^*})^{\phi+1} + (A q_{o^*}^2 - B q_{o^*} + C)(x_* + q_{o^*})^{\phi}\right](x_* + q_{o^*})^{-\phi} + K(x_* + q_{o^*})^{-\phi} \tag{22}$$

The constant of integration, K, can be obtained by imposing the boundary conditions that at the upper edge of a deposition region $x_* = x_{u^*}$ and nondimensional sediment load $G^* = G^*_u$. Using this substitution, the constant K is equal to:

$$K = (x_{u^*} + q_{o^*})^{\phi}\left[G^*_u - \frac{\phi A}{\phi + 2}(x_{u^*} + q_{o^*})^2 - \frac{(\phi B + \theta - 2A\phi q_{o^*})}{\phi + 1}(x_{u^*} + q_{o^*}) - (A q_{o^*}^2 - B q_{o^*} + C)\right] \tag{23}$$

Equation 22 can be solved for individual particle classes. To do this, several of the variables must be partitioned into values for the individual classes. The interrill detachment parameter, θ, is partitioned based on the predicted fraction of sediment in each size class reaching the rill channel, $fidel_i$, as computed in equation 9. The deposition parameter, θ, is computed for each particle class, using the individual class diameter and specific gravity, and a value of 0.5 is assumed for β. The dimensionless transport coefficients A, B, and C, are proportioned for each particle class based on fractions of transport capacity computed

using the Yalin (1963) transport equation when the input shear stress is the average of the shear stresses calculated using the actual slope and the average slope for the OFE.

The fraction of sediment in each size class at the top of a depositional region is computed using a simple mass balance:

$$f_{enddet}(i) = \frac{f_{topdet}(i) G^*_{topdet}}{G^*_{enddet}} + \frac{f_{deti}\left(G^*_{enddet} - G^*_{topdet} - fidel_i\,\theta\left(x_{enddet^*} - x_{topdet^*}\right)\right)}{G^*_{enddet}} \quad (24)$$

where f_{enddet} is the fraction of sediment in size class i at the end of the last detachment region and beginning of the current deposition region, f_{topdet} is the fraction of sediment in size class i at the beginning of the last detachment region, x_{topdet^*} is the nondimensional distance from the top of the OFE to the top of the last detachment region, x_{enddet^*} is the nondimensional distance from the top of the OFE to the end of the last detachment region, G^*_{topdet} is the normalized sediment load at the beginning of the last detachment region, and G^*_{enddet} is the normalized sediment load at the end of the last detachment region. The sediment size class fractions in the flow must be updated each time a new depositional region is reached, and at the end of an overland flow element.

In the current WEPP enrichment subroutine, equation 22 is used to calculate a sediment load for each size class at the end of the depositional region. The $G^*_e(i)$ values are summed and each $G^*_e(i)$ is multiplied by the ratio of the end region sediment load divided by the sum of the $G^*_e(i)$. This correction assures that the load at the end of the region is the same as that computed in the total sediment load computations.

Next, a test is made to determine if $G^*_e(i)$ exceeds the maximum sediment load limit, $G^*_{e\,max}(i)$, calculated as:

$$G^*_{e\,max}(i) = G^*_u(i) + \theta_i\left(x_{e^*} - x_{u^*}\right) \quad (25)$$

In other words, the sediment load at the end of a depositional region cannot be larger than the incoming sediment load plus the interrill contribution between x_{u^*} and x_{e^*}. WEPP assumes that only deposition can occur from x_{u^*} to x_{e^*} (no rill detachment is allowed in any size class).

If $G^*_e(i)$ is greater than $G^*_{e\,max}(i)$, the sediment load at the end of the depositional region for the ith size class is set equal to the maximum allowable. The excess load is then reassigned to the remaining classes. This is done by giving each unfilled class additional load based on its original computed load at x_{e^*}. For example, if three of the five particle classes have reached their maximum possible loads, and the remaining two classes were originally predicted to make up 20% and 10% of the total load at x_{e^*} (classes 4 and 5, respectively), then two-thirds of the excess sediment load would be shifted to the fourth class, and one-third of the excess would be shifted to the fifth class. This method was selected because it partially retains some of the particle size distribution information obtained when equation 22 is solved for each size class. The end result of the incorporation of the entire equation set into WEPP is that the model can rapidly predict the size fractions of sediment leaving a depositional region (though no information on different particle size deposition locations within a region is provided). In general, more fine sediment will be predicted to reach the end of a deposition region than will coarser particles.

At the end of each overland flow element, an enrichment ratio of the sediment is computed using a relationship from the CREAMS model (USDA, 1980):

$$ER = \frac{SSA_{sed}}{SSA_{soil}} \quad (26)$$

where ER is enrichment ratio, SSA_{sed} ($m^2 \cdot g^{-1}$) is the total specific surface area of the sediment in the flow exiting an element, and SSA_{soil} ($m^2 \cdot g^{-1}$) is the specific surface area of the *in situ* soil. The value of SSA_{sed} is calculated using:

$$SSA_{sed} = \sum_{i=1}^{5} f_{out}(i) \times \left[\frac{frsnd(i)\,ssasnd + frslt(i)\,ssaslt + frcly(i)\,ssacly}{1 + frorg(i)} + \frac{frorg(i)\,ssaorg}{1.73}\right] \quad (27)$$

where frsnd(i), frslt(i), frcly(i), and frorg(i) are the fractions of sand, silt, clay, and organic matter comprising each particle class, respectively, and ssasnd, ssaslt, ssacly, and ssaorg are the specific surface area for sand, silt, clay, and organic carbon, respectively. Values for the specific surface area used in the model computations are 0.05, 4.0, 20.0, and 1000.0 $m^2 \cdot g^{-1}$ of sand, silt, clay, and organic carbon, respectively, as used in CREAMS (Foster et al., 1980a).

The value for SSA_{soil} is computed using:

$$SSA_{soil} = \frac{orgmat(ssaorg)}{1.73} + \frac{sand(ssasnd) + silt(ssaslt) + clay(ssacly)}{1 + orgmat} \quad (28)$$

where sand, silt, clay, and orgmat are the fractions of sand, silt, clay, and organic matter in the surface soil, respectively.

The WEPP computer program calculates the particle size distribution in the rill flow at the beginning and end of each depositional region, and an enrichment ratio at the end of each overland flow element. For a single storm simulation, model output contains information on particle size, composition, detached sediment fraction, and fraction in the rill flow exiting the hillslope. The sediment enrichment ratio is also printed. In a continuous model simulation over a number of years, mass fraction in each particle size class and enrichment ratio is weighted for each storm event by the total sediment discharge for the event.

The particle information, weighted fractions, and weighted enrichment ratio are then output in a format identical to that for the single storm results.

Model Response

Single storm simulations of WEPP model version 98.4 were conducted to examine the effects of soil type, slope gradient, slope shape, slope length, rainfall intensity, and random roughness on particle sorting and sediment enrichment ratio. Both interrill and rill effects were examined. This exercise was meant to display the functionality and range of results possible with WEPP. Six base soil types used in the analyses were a sand (90% sand, 5% silt, 5% clay), a loam (40% sand, 40% silt, 20% clay), a silt loam (5% sand, 75% silt, 20% clay), a silty clay (5% sand, 65% silt, 30% clay), a silt (5% sand, 90% silt, 5% clay), and a clay (20% sand, 20% silt, 60% clay). Base organic matter content for all soils was set at 2%, CEC was 10 meq/100 g, rock fragments were 1%, albedo was 0.20, and initial saturation was 75%. The soil was assumed to be in a bare, fallow condition with no residue or plant cover. Internal computations within WEPP were used to compute effective hydraulic conductivity based upon the input soil properties. Erodibilities for all soils were set to constant values of 2 000 000 $kg \cdot s \cdot m^{-4}$ for interrill erodibility, 0.003 $s \cdot m^{-1}$ for rill erodibility, and 3.3 Pa for critical shear. Base values were held constant with only the other variables of interest being changed. The implication of using this procedure is that it will show trends rather than extreme results that could occur from some odd combination of inputs.

Interrill Processes

From equations 3 to 9, sediment particle sorting on interrill areas results in size fractions delivered to rill channels that are mostly a function of random roughness. The base design storm for the interrill trials was 100 mm of rainfall in 4 h, with a time to peak of 0.5 and ratio of peak to average intensity of 2. The base hillslope profile was 50 m long with a uniform 1% slope gradient. Rill spacing was set at 1.0 m and ridge height at 0.05 m. The storm and slope characteristics were selected based upon multiple runs of the WEPP model, which showed that for most cases on all of the soils used, no additional sediment would be added to the rill flow by rill detachment or removed from the rill flow by deposition. Variations in output sediment size distributions and enrichment ratio would thus be due solely to interrill particle sorting. Random roughness was varied from 6 to 49 mm, and the results are presented in figures 2-4.

Figure 2 shows the relationship between event runoff and random roughness for the six soils. The silt loam and clay soils have the highest runoff amounts, the silt and silty clay soils have moderate levels of runoff, and the loam and sand soils have the least runoff. These results are due to the equations used internally within WEPP to compute effective hydraulic conductivity, with more soil sealing and crusting predicted for the soils composed of higher amounts of silts and clays (Alberts et al., 1995). Figure 2 also shows a trend of decreasing runoff depth with greater random roughness, which is due to greater depressional storage predicted by WEPP for rougher surfaces.

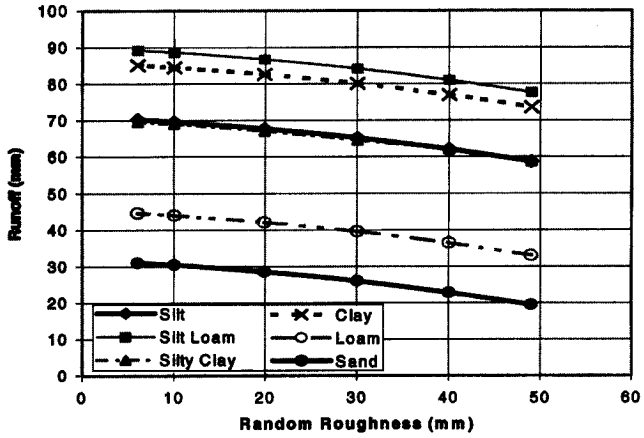

Figure 2–Model predicted runoff depth versus random roughness for the six different soil types from a single storm of 100 mm over a period of 4 h.

Sediment yield from the single storm simulations was also highly dependent upon soil type and random roughness (fig. 3). Sediment yield was highest at the lowest values of random roughness, and the silt loam, clay, silty clay, and silt soils all had similar values for sediment yield (between 20 and 30 kg/m). Sediment yield for the loam and sand soils was much lower, due to decreased runoff as well as to having fewer transportable sediment particles. As random roughness was increased, sediment yield decreased for all soil types, though losses from the silt soil were relatively much higher than those from the other soils, due to a larger fraction of easily transported primary silt predicted for this soil.

Specific surface area enrichment ratio of the sediment leaving the 50-m-long hillslope profiles is shown in figure 4. At the minimum random roughness value of 6 mm, all sediment predicted to be detached from the interrill areas is transported to the rill channels and off the slope, thus the enrichment ratio is 1.0. The exception was the sand soil for which some deposition was predicted in the rill channel in the simulations with random roughness at levels of 6 and 10 mm, yielding an enrichment ratio of slightly greater than 1.0. As random roughness increased,

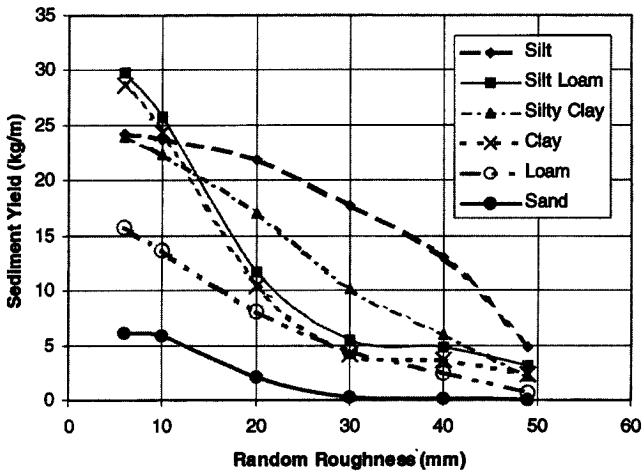

Figure 3–Model predicted sediment yield versus random roughness for the six different soil types from single storm WEPP simulations.

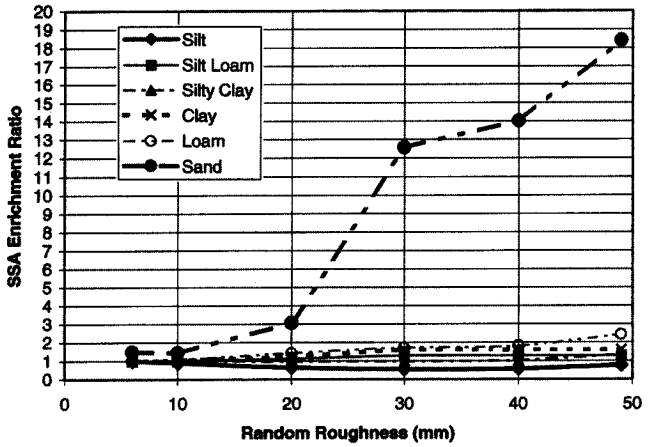

Figure 4–Model predicted Specific Surface Area (SSA) enrichment ratio versus random roughness for the six different soil types.

the enrichment ratio increased from 1.0 as more particle sorting on the interrill areas was predicted. For the sand soil, the ratio became extremely high (approaching 19), due to all sediment leaving the interrill areas and hillslope being primary clay, primary silt, and small aggregates, and due to the relatively low specific surface area of the *in situ* soil (denominator of eq. 26).

Rill Enrichment Ratio

For the simulations examining the sediment enrichment ratio as affected by rill deposition/detachment processes, the base design storm was 100 mm of rainfall in 2 h, with a time to peak of 0.5 and ratio of peak to average intensity of 2. The base hillslope profile was 50 m long with a uniform 1% slope gradient. Rill spacing was 1.0 m, ridge height was 0.05 m, and random roughness was 20 mm. Several test simulations were conducted to examine the impact of changes in soil type, slope shape, slope gradient, slope length, and rainfall/runoff intensity. The results are presented in figures 5-8.

Soil texture had a very large impact on enrichment ratio (fig. 5). At the lowest slope values, the sand soil had the highest predicted enrichment ratio, exceeding 6.0 at a slope of 0.25%. High enrichment ratio values for sand are due to several factors, including relatively lower amounts of runoff predicted, very high fractions of primary clay and silt predicted in the outflow sediment, and a relatively low amount of specific surface area in the *in situ* soil. The other five soil types had enrichment ratios that fell within the range of 0.6 to 1.6 for the base test situation (slope of 1%). The largest deviations from a value of 1.0 (which indicates no particle sorting or enrichment) occurred at the lowest slope values, and as average slope gradient increased, enrichment ratio for all soils approached 1.0.

In some cases, enrichment ratio may be less than one. For example, soils with large amounts of silt exhibited this behavior in most simulations (figs. 4 and 5). The aggregates of these soils are predicted to contain significant amounts of the clay and organic matter present in the soil. There is also a sizable portion of primary silt in the detached sediment. If conditions are favorable for selective deposition of the small and large aggregates, the fraction of primary silt can be greatly enriched. Since silt has a much lower specific surface area than the clay and organic matter in the aggregates, the total specific surface area of the sediment is reduced below that of the soil, causing the enrichment ratio to become less than 1.0.

Slope shape also greatly affected the predicted particle sorting. Figure 6 depicts the impact of various slope shapes on enrichment ratio for the sand soil. A convex shape had a slope of zero at the top and a slope twice the average slope at the bottom. A concave shape had a slope of zero at the bottom and a slope twice the average slope at the top. An S-shaped profile had a slope of zero at the top and bottom, and a slope of twice the average slope at the center. The concave and S-shaped profiles resulted in much greater predicted particle sorting and enrichment ratios, due to the zero slope conditions at the end of the profile, forcing rill deposition. As the average slope gradient was increased, enrichment ratio remained between two and three. For the uniform and convex slopes, predicted deposition in the rills on the profile decreased with increasing slope gradient, and approached a value of one.

Figure 7 shows the impact of slope length and slope gradient on enrichment ratio for a sand soil. Here, slope lengths of 10 m, 50 m, and 100 m were used in the simulations, while all other parameters were set at base levels, except slope gradient which was varied from 0.25 to 20%. At the lowest slope gradients, all three slope lengths resulted in similar particle sorting and enrichment ratios.

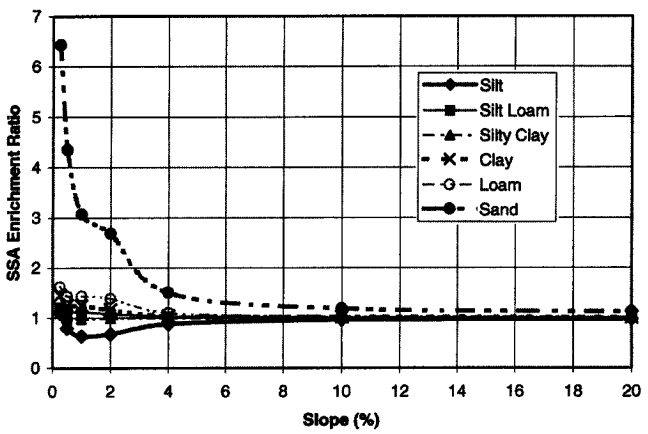

Figure 5–SSA Enrichment Ratio predicted by WEPP ver. 98.4 for a uniform slope profile as a function of soil texture and slope gradient.

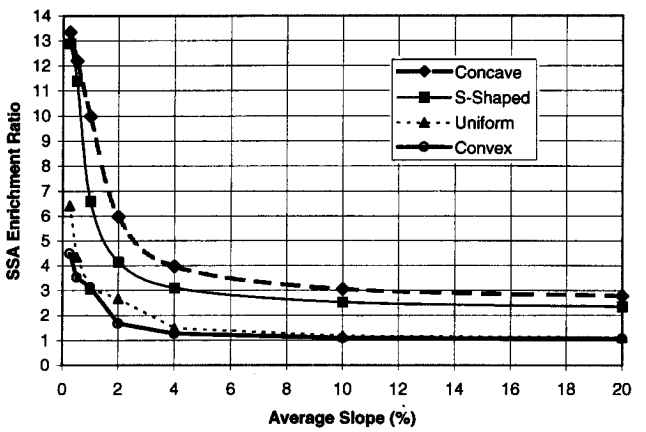

Figure 6–SSA Enrichment Ratio predicted by WEPP v98.4 for a sand soil as a function of slope shape and average slope gradient.

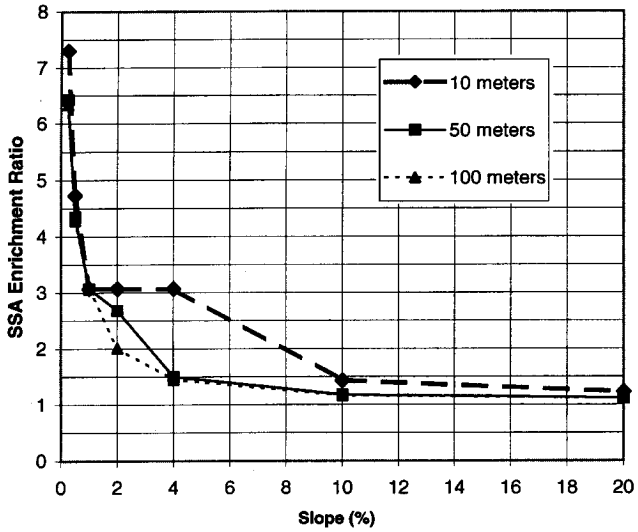

Figure 7–SSA Enrichment Ratio predicted by WEPP ver. 98.4 for a uniform hillslope profile on a sand soil as a function of slope length and gradient.

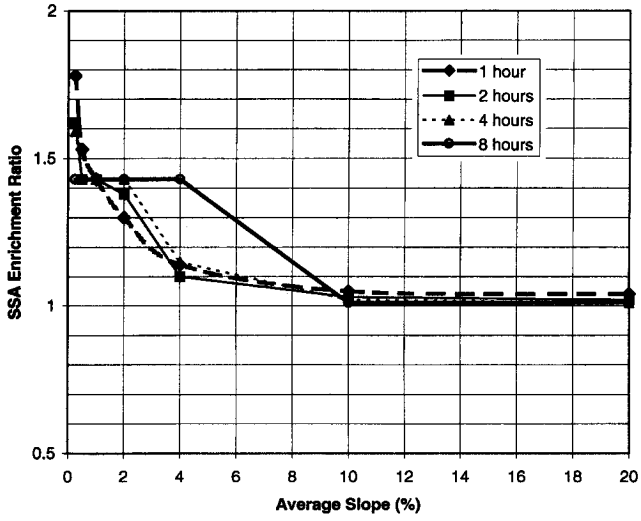

Figure 8–SSA Enrichment ratio predicted by WEPP ver. 98.4 for a uniform hillslope profile on a loam soil as affected by rainfall (and runoff) intensity (lines represent varying durations of rainfall).

This was because the uniform slope rill channel was in a depositional mode and received the same sediment from the interrill areas (which was itself enriched due to the random roughness value of 20 mm, see fig. 4). However, as slope gradient increased, rill detachment began to influence the results. For the long 100 m slope length, as the gradient increases a large amount of sediment delivered from the profile originates from detachment in the rill, so the enrichment ratio rapidly approaches a lower value. For the short (10 m) slope, rill detachment is limited, so much of the sediment delivered from the rill still originates on the interrill areas (and has a greater fraction of fine particles). The 50-m-long profile has results between the two extremes.

Rainfall and resulting runoff intensity can also affect the predicted particle sorting and enrichment. For these set of simulations, rainfall depth was kept constant at 100 mm while rainfall duration was varied from 1 to 8 h (for the sand soil, the 8 h duration resulted in zero runoff and sediment yield). Figure 8 shows the impact of the changes in rainfall and associated runoff intensities and slope gradient on enrichment ratios for the loam soil. At the highest slope gradients, the highest intensity storm always had a minimally larger value of enrichment ratio across all soil types. However, at low and moderate slope values, particle sorting and enrichment results were very complex. In figure 8, as slope was varied from 0.25% to 10%, the effect of rainfall intensity changed twice, due to the effects which rainfall intensity has on both interrill and rill detachment rates. These results of the effect of storm intensity on enrichment ratio also provide some insight into the practical implications for users concerned with sediment delivery in real world situations. In many instances, a relatively few large storm events are responsible for the majority of soil loss and sediment yield from a hillslope, and in situations such as this it is possible that little sorting of sediment will occur and the sediment leaving a profile will be quite similar to that at the point of detachment upslope.

VALIDATION STUDY

A validation study was conducted using WEPP model version 98.4 and data from three previous field experiments covering a range of flow and deposition conditions. The main purpose of the validation effort was to determine if the enrichment equations implemented in WEPP could adequately represent the particle sorting observed under some field conditions. Due to the nature of the available data, the major relationships tested were those for rill sediment particle fraction prediction. The three experiments covered a wide range of sediment deposition conditions, including deposition of sediment generated upslope in a slope concavity, deposition of sediment generated on row side ridges in a low uniform slope gradient furrow, and deposition induced by a large decrease in transport capacity caused by a grass filter strip on a uniform steep slope.

The first data set was from a concave plot experiment conducted near West Lafayette, Indiana, in the summer of 1977 (Foster et al., 1980b). Concave plots 10.7 m long were formed in a uniform subsoil, with the slope decreasing continuously from 18% at the top to 0% at the bottom. Simulated rainfall was applied at a uniform intensity of 64 $mm \cdot h^{-1}$. The first plot was used to determine that deposition began 7 m from the top. Plot ends were then placed at 7 and 8.8 m on the other two plots. The data collected from the three plots included the sediment amount and size distribution entering the deposition region, and the sediment amount and size distribution at two points within the deposition region.

The WEPP computer model was used to simulate these field concave plots. Input infiltration parameters were adjusted to give the observed runoff rates, and erodibility parameters were adjusted so that deposition was predicted to begin at the observed location of 7 m. The WEPP model was altered to allow input and use of the observed sediment size fractions entering the deposition region, instead of using the relationships of Foster et al. (1985). The predicted sediment size fractions exiting the plots were then compared to the observed values.

Results of the two simulations of the field concave experiment are presented in figures 9 and 10. Predicted sediment size exiting the 10.7-m-long slope closely matched the observed values (fig. 9). For the 8.8-m-long slope, WEPP predicted somewhat lower values for the large size fractions than were actually observed in the experiment (fig. 10). A linear regression was conducted using the sixteen-paired values of observed and predicted size fractions (fig. 11), and the coefficient of determination (r^2) was 0.97. Overall, the rill sediment enrichment functions predicted exiting size fractions that closely matched the observed values.

The second set of validation data was from a study by Meyer and Harmon (1985) on ridge-furrow plots in Mississippi on a Loring silt loam soil. They applied simulated rainfall at rates of 27, 71, and 106 mm·h^{-1} to 9.3 m × 0.97 m bedded rows having furrow gradients of 0.5, 2.0, 3.5, 5.0, and 6.5%. Since they only observed rill deposition on the lowest slope gradient, this validation exercise used only those data. The input hydrology parameters to the WEPP model were adjusted to give the observed runoff rates from the plots. Input model interrill

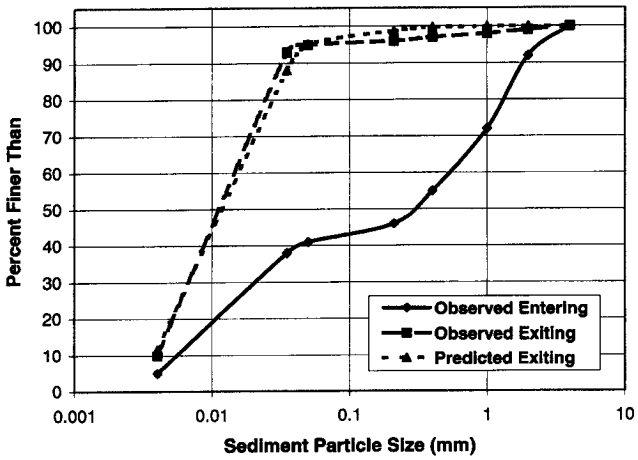

Figure 9–Particle size distributions for concave field plot experiment (Foster et al., 1980b) in which slope decreased from 18% to 0% over a distance of 10.7 m.

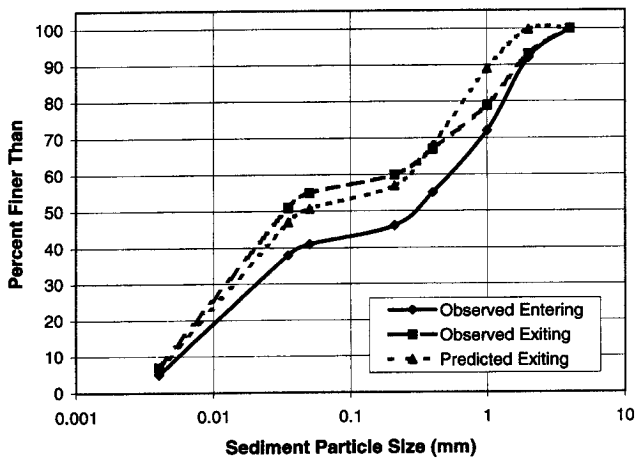

Figure 10–Particle size distributions for concave field plot experiment (Foster et al., 1980b) in which slope decreased from 18% to 3% over a distance of 8.8 m.

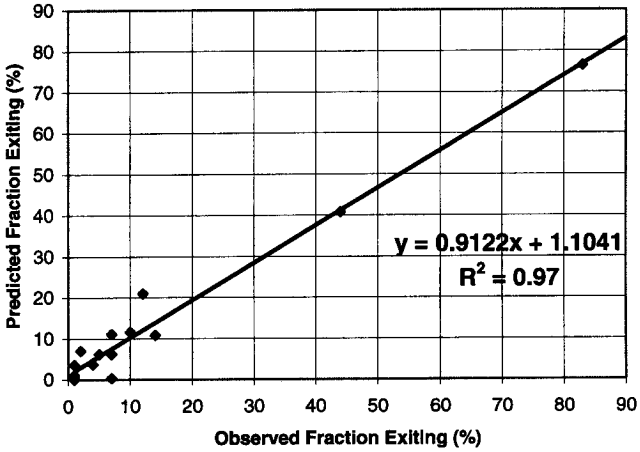

Figure 11–Predicted versus observed sediment size fractions exiting the 8.8 m and 10.7 m long concave plots of Foster et al. (1980b).

erodibility was adjusted to give the interrill detachment observed on small 0.91 m × 0.97 m companion plots. The particle size fractions from these row sideslope plots were also used as the input detached sediment fractions for the WEPP model. There were two replicates of four experimental runs: an initial run on dry soil at 71 mm·h^{-1}, and runs on wet soil at 27, 71, and 106 mm·h^{-1}. Changes were made in the WEPP model input value for rill cover so that predicted sediment leaving the furrows could be matched to observed sediment leaving the furrows as closely as possible. The predicted and observed sediment size fractions were then compared.

Results of the simulations are presented in figure 12. A linear regression performed between observed and predicted size fractions over all 10 size classes, four runs, and two replications yielded a coefficient of determination (r^2) value of 0.75. Figure 13 shows the average values of the size fractions for the observed incoming sideslope sediment, observed sediment exiting the furrows, and for the WEPP model predicted sediment exiting the furrows over all rainfall intensity levels. In general, the WEPP model predicted most size fractions fairly well, with the

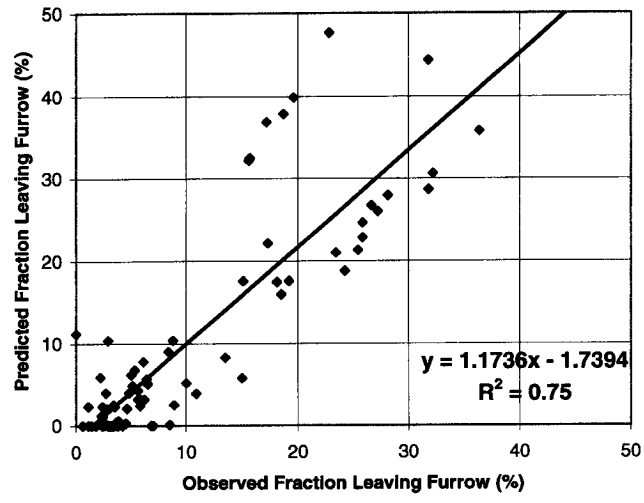

Figure 12–Predicted versus observed sediment size fractions for Meyer and Harmon (1985) data. Values plotted are for ten size classes from two replicates of four runs on furrows at 0.5% slope gradient over all rainfall intensities.

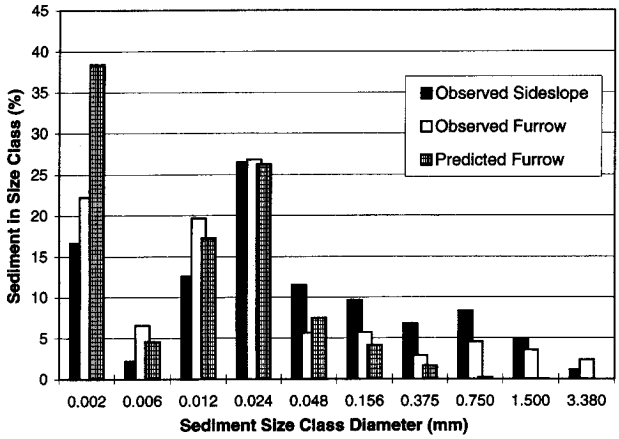

Figure 13–Average observed and predicted sediment size classes exiting the ridge furrow plots of Meyer and Harmon (1985) at a slope gradient of 0.5% over all rainfall intensities.

exception of the primary clay fraction, which was consistently overpredicted, and the aggregates 0.75 mm and larger, which were consistently underpredicted. In the observed furrow particle data, primary clay fraction was often close to that of the observed incoming sideslope plots, indicating no clay enrichment. In addition, the observed exit values for the large aggregate classes were close to (or even exceeded) the observed incoming sideslope values. It is not clear why the observed clay and large aggregate data exhibited this unexpected behavior. One possible explanation is that field erosion experiments with ridge-furrows on very low slopes have active deposition that with time can substantially change the flow exit conditions (slope, shear, transport capacity), and this might have enhanced the transport of the larger aggregates.

The third set of experimental data used in validation was from a study by Neibling and Alberts (1979), in which simulated rainfall was applied to a bare silt loam soil above sod strips. Simulated rainfall was applied at a target intensity of 64 mm·h^{-1} to 6 m × 3.6 m plots at a uniform slope of 7%. The plots were split so that half of the runoff and sediment flowed into grass strips of 0.6, 1.2, 2.4, and 4.9 m length, and the other half of the runoff and sediment was measured to give the sediment amount and size distribution entering the strips. The particle size fractions exiting the bare soil were set to be those for the detached soil in the WEPP model. Input infiltration and erodibility parameters for WEPP were adjusted so that runoff and soil loss rates matched the observed values as closely as possible. WEPP model version 98.4 was altered to allow adjustment of the total load deposition rate, so that the predicted total sediment leaving the strips could be matched as closely as possible to the observed total sediment loss values. In some cases it was not possible to match extremely low sediment loss values from the sod, and in these situations the total load deposition rate was manipulated so that the predicted fraction of primary clay matched as closely as possible to the observed value. Model predicted particle size fractions exiting the grass strips were then compared to those observed in the experiment. Only 14 runs from this study (six on initially dry soil and eight on very wet soil) contained all of the observed particle size data necessary to conduct the simulations.

Results of the sod strip analyses are presented in figure 14. The coefficient of determination between the observed and predicted size fractions was r^2 = 0.44. Figure 15 shows the mean values for the observed and predicted size over all of the runs. In general the WEPP model correctly predicted the trends of the enriched sediment size distribution, but tended to underpredict the smallest size fractions (clay and silt), and overpredict most of the medium size fractions. One of the reasons for the poorer model performance probably has to do with the physical processes occurring on the actual experimental plots, and how WEPP is attempting to simulate them. Photographs of the sod strip plots during an experiment showed that sediment-laden water was ponded for 0.5 to 1.0 m above the grass, thereby providing an opportunity for substantial deposition and particle enrichment. WEPP hillslope model simulations do not account for backwater effects, and only predict decreases in sediment transport

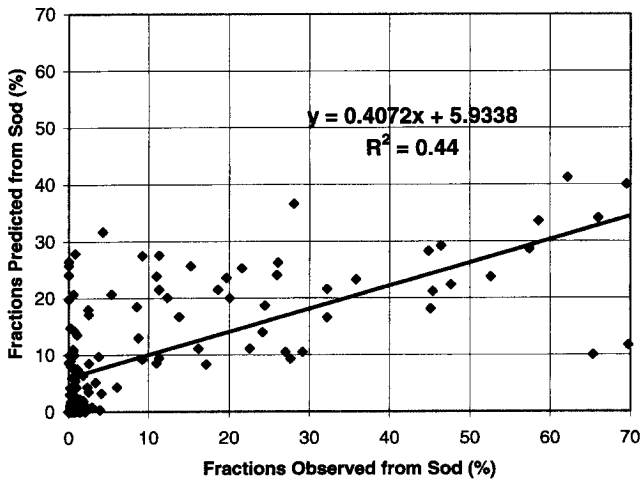

Figure 14–Predicted versus observed size fractions for Neibling and Alberts (1979) data. Values plotted are for 10 size classes over all strips lengths, soil moisture conditions, and replications.

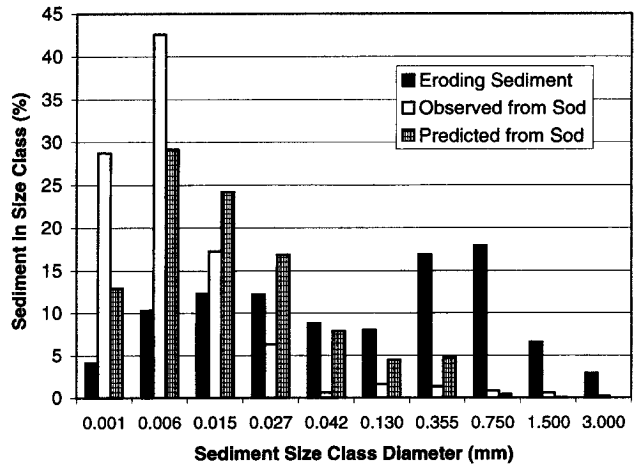

Figure 15–Average observed and predicted sediment size classes for the study of Neibling and Alberts (1979). Values plotted are for 10 size classes over all strips lengths, soil moisture conditions, and replications.

capacity and subsequent deposition in the more hydraulically rough sod region.

DISCUSSION

Very few data exist to validate the particle sorting procedures described here. In the limited validation study conducted for this article, the enrichment routines reproduced the general trends observed, although they did not always do a satisfactory job of matching size fractions in each particle size class. Extensive comparison testing between the WEPP model deposition and particle sorting calculations and those predicted with the CREAMS model (USDA, 1980) has been proposed to determine if the current WEPP procedures for estimating sediment deposition, particle sorting and sediment enrichment are adequate or if improvements are warranted. Computer resources are no longer the limiting factor that they were during the initial development of WEPP, so changes in the WEPP detachment and deposition computations which require more calculations at points down a hillslope profile may be justified and more readily implemented. Results in an unpublished preliminary evaluation between WEPP and CREAMS techniques conducted in late 1994 indicated that the two models can predict greatly different locations of deposition for a concave slope scenario. More in-depth studies to compare CREAMS and WEPP deposition techniques need to be conducted in the future.

The approach described in this article for predicting particle sorting on interrill and rill areas during a WEPP model simulation has several advantages. The WEPP erosion model was written to predict sediment loss on a total load basis (Nearing et al., 1989; Foster et al., 1995), and the addition of these routines has allowed independent prediction of particle size distributions under the assumption that the total load estimates of sediment deposition are correct. The equations described here are computationally efficient and require very few computer resources, in comparison to other techniques. The approach is relatively simple as implemented in the computer code, and there are minimal solution convergence problems found in alternative numerical methods.

The approach described here also has some disadvantages. The equations require that the depositional regions have already been determined by the model, and as implemented do not allow for any correction to the total sediment load values computed in the rills based upon values calculated for the individual size classes with equation 22. A major concern lies in the use of an effective particle fall velocity to predict the total load estimates of sediment deposition, particularly for soils having very high fractions of sand and large aggregate particles compared to clay, silt, and small aggregates. Additionally, the interrill delivery function (eq. 2) is not truly process-based, and does not explicitly determine the interrill sediment detached, transported, and deposited during a runoff event.

Another problem is that overland flow elements may be composed of variable soil types for which the model may predict greatly different detached soil particles. Highly variable adjacent soil types could cause large differences in the prediction of the particle classes, particularly in the size of the primary sand and large aggregates, the composition of both aggregate classes, and the detached fractions of all classes. On a given OFE, the model will use the characteristics of the current OFE's soil to determine the sediment deposition parameters in equation 16 used in equation 22, as well as the soil factor values in equations 26-28. The WEPP enrichment routines will function in these situations, but the predictions at the end of the downslope flow elements may be in error. However, fewer problems would be expected if there are no significant deposition regions on the hillslope (ER $\approx$ 1.0) or if a significant amount of detachment occurs somewhere within the last slope element, again forcing ER to approach 1.0.

SUMMARY AND CONCLUSIONS

This article describes the equations and approach used to model sediment particle sorting on interrill areas and during rill deposition that are currently implemented in the USDA-ARS Water Erosion Prediction Project (WEPP) computer program. Predicted sediment size distributions and the resulting sediment enrichment ratios can be greatly affected by soil type, random roughness, slope shape, slope gradient and slope length. Storm intensity alters interrill detachment and rill runoff rates, so it can also affect sediment enrichment. The WEPP model predicts sediment enrichment ratios varying across a range from 0.6 to more than 18. Very high enrichment ratios can occur on sandy soils for which large amounts of deposition of the coarse sand are predicted and for which the transported sediment is largely primary clay and silt. Enrichment ratios less than 1.0 can occur for soils having large fractions of primary silt, in which case selective deposition of aggregates composed of sediment particles with greater specific surface area results in relatively larger fractions of primary silt sediment that has a lower specific surface area than the *in situ* soil. For all soil types, as the erosion process shifts from a depositional mode to a detachment mode, enrichment ratios will approach a value of 1.0.

A limited validation study using data from three field experiments was conducted to examine the performance of the WEPP approach. The data covered conditions of deposition on a concave slope, deposition in a ridge-furrow system, and deposition caused by a grass filter strip. Coefficients of determination (r^2 values) in linear regressions comparing observed and predicted sediment size fractions were 0.97, 0.75, and 0.44 for data from the three experiments, respectively. One likely reason for poorer performance for the grass filter strip data was the presence of ponded water behind the strips that enhanced deposition of medium-sized particles and increased the fractions of fine silt and clay sediment. This effect of backwater is not currently modeled in WEPP hillslope simulations. Overall, the validation study showed that the current WEPP equations can approximate observed trends in particle size data, although predictions in individual classes may sometimes be poor.

ACKNOWLEDGMENTS. The authors wish to acknowledge George Foster for insight and suggestions on approaches for estimating interrill sediment particle sorting. They would also like to thank Don Meyer, William Harmon, and Howard Neibling for providing detailed data from their field experiments for use in the validation study.

REFERENCES

Alberts, E. E., M. A. Nearing, M. A. Weltz, L. M. Risse, F. B. Pierson, X.C. Zhang, J. M. Laflen, and J. R. Simanton. 1995. Ch. 7. Soil component. In *USDA—Water Erosion Prediction Project (WEPP) Hillslope Profile and Watershed Model Documentation*, eds. D. C. Flanagan, and M. A. Nearing. USDA-Agricultural Research Service, NSERL Report No. 10. West Lafayette, Ind.: National Soil Erosion Research Laboratory.

Finkner, S. C., M. A. Nearing, G. R. Foster, and J. E. Gilley. 1989. A simplified equation for modeling sediment transport capacity. *Transactions of the ASAE* 32(5): 1545-1550.

Flanagan, D. C., and M. A. Nearing, ed. 1995. *USDA—Water Erosion Prediction Project (WEPP) Hillslope Profile and Watershed Model Documentation.* USDA-Agricultural Research Service, NSERL Report No. 10. West Lafayette, Ind.: National Soil Erosion Research Laboratory.

Foster, G. R. 1982. Modeling the erosion process, Ch. 8. In *Hydrologic Modeling of Small Watersheds*, eds. C. T. Haan, H. P. Johnson, and D. L. Brakensiek. St. Joseph, Mich.: ASAE.

Foster, G. R., L. J. Lane, and J. D. Nowlin. 1980a. A model to estimate sediment yield from field-sized areas: Selection of parameter values, Ch. 2. In *CREAMS—A Field Scale Model for Chemicals, Runoff, and Erosion From Agricultural Management Systems*, 193-281, ed. W. G. Knisel. USDA Cons. Res. Report No. 26. Washington, D.C.: USDA-SEA.

Foster, G. R., W. H. Neibling, S. S. Davis, and E. E. Alberts. 1980b. Modeling particle segregation during deposition by overland flow, 184-195. In *Proc. Hydrologic Transport Modeling Symposium.* St. Joseph, Mich.: ASAE.

Foster, G. R., R. A. Young, and W. H. Neibling. 1985. Sediment composition for nonpoint source pollution analyses. *Transactions of the ASAE* 28(1): 133-139.

Foster, G. R., and L. J. Lane. 1987. User requirements, USDA-Water Erosion Prediction Project (WEPP). NSERL Report No. 1. West Lafayette, Ind.: National Soil Erosion Research Laboratory.

Foster, G. R., D. C. Flanagan, M. A. Nearing, L. J. Lane, L. M. Risse, and S. C. Finkner. 1995. Hillslope erosion component, Ch. 11. In *USDA—Water Erosion Prediction Project (WEPP) Hillslope Profile and Watershed Model Documentation*, eds. D. C. Flanagan, and M. A. Nearing. USDA-Agricultural Research Service, NSERL Report No. 10. West Lafayette, Ind.: National Soil Erosion Research Laboratory.

Meyer, L. D., and W. D. Harmon. 1985. Sediment losses from cropland furrows of different gradients. *Transactions of the ASAE* 28(2): 448-453, 461.

Nearing, M. A., G. R. Foster, L. J. Lane, and S. C. Finkner. 1989. A process-based soil erosion model for USDA-water erosion prediction project (WEPP) technology. *Transactions of the ASAE* 32(5): 1587-1593.

Neibling, W. H., and E. E. Alberts. 1979. Composition and yield of soil particles transported through sod strips. ASAE Paper No. 79-2065. St. Joseph, Mich.: ASAE.

Pennisi, L. L. 1972. *Elements of Ordinary Differential Equations*, 78. New York, N.Y.: Holt, Rinehart & Winston, Inc.

United States Department of Agriculture. 1980. *CREAMS—A Field Scale Model for Chemicals, Runoff, and Erosion from Agricultural Management Systems*, ed. W. G. Knisel. USDA Cons. Res. Report No. 26. Washington, D.C.: USDA-SEA.

Wischmeier, W. H., and D. D. Smith. 1978. Predicting rainfall erosion losses—A guide to conservation planning. Agricultural Handbook No. 537. Washington, D.C.: U.S. Department of Agriculture.

Yalin, M. S. 1963. An expression for bed-load transportation. *J. Hydr. Div.*, ASCE 98(HY3): 221-250.